

## Creation and Evaluation of a Polyurethane/Carbon/Zinc Oxide Film Composite for Use as a Coating Material

Ova Kurniawan<sup>1\*</sup>, Bambang Soegijono<sup>2</sup>

<sup>1</sup> Department of Electrical Engineering, Institut Teknologi Perusahaan Listrik Negara, Jakarta, 11750, Indonesia.

<sup>2</sup> Mathematics and Natural Sciences Faculty, Institut Sains dan Teknologi Nasional, Jakarta, 12630, Indonesia.

\* Corresponding Author. E-mail : [ova@itpln.ac.id](mailto:ova@itpln.ac.id)

Article information - : Received : 28-05-2025; Revised : 27-06-2025; Accepted : 24-07-2025

### Abstract

*The material used as a coating must have unique characteristics. A frequently used coating material is polyurethane. Even though polyurethane has been widely used as a coating material, it has limitations in thermal resistance. Incorporating fillers such as carbon and ZnO can improve its thermal, dielectric, and corrosion-resistant properties. Composite films of polyurethane with carbon, ZnO, and a mixture of both were prepared. Characterizations included FTIR, TGA, DSC, XRD, dielectric testing, salt spray, water vapor permeability, hydrophobicity, and adhesion tests. FTIR confirmed the presence of functional groups from the fillers. TGA and DSC showed improved thermal stability, particularly in carbon-filled composites. Salt spray and permeability tests indicated enhanced corrosion resistance in ZnO-filled samples, while dielectric properties improved with carbon addition. Hydrophobicity and adhesion tests met coating material criteria. Among all variants, the polyurethane/carbon composite demonstrated the most favorable combination of thermal, dielectric, and surface properties, making it the most suitable for protective coating applications.*

**Keywords:** dielectric; thermal resistance; corrosion resistance; composite; polyurethane.

### 1. Introduction

The use of coating materials to protect and increase the life of a material is commonly used. Some of the purposes and objectives of using specific coating materials are to prevent corrosion, withstand heat and various other things. The material used as a coating must have unique characteristics such as polyurethane. Application of polyurethane as a multipurpose material has been widely used in various fields and naturally be easily adjusted both physically and chemically by certain additives to desired properties [1], [2]. However, polyurethane also has several obstacles, especially related to the nature of thermal resistance properties [3]– [5]. Additives can be added to polyurethane including carbon and zinc oxide. Some research has investigated polyurethane and carbon composites to obtain mechanical properties and water permeability which addition of carbon can improve mechanical strength and resistance to fire by 20% by adding as much as 0.05% carbon to polyurethane [6], [7]. Along with the developments made by the researchers, nano sized ZnO has become a filling material that has many advantages. This is because the very small particle size (nanometer) makes the surface interactions occur between nano-fillers and the polymer matrix become stronger. Therefore, it can improve the performance of the properties and uses of polymers. ZnO nanoparticles have been utilized as fillers in a variety of polymers, including polyethylene, polypropylene, polystyrene, and more recently, polyurethane, in order to attain their characteristic performance (corrosion and heat resistance, mechanical capabilities, and thermal properties) for specific applications [8].

The objective of this study is to perform a comprehensive characterization of polyurethane composites incorporating carbon and zinc oxide fillers, with the aim of assessing their potential application as protective coating materials.

The novelty of this study lies in the comparative characterization of polyurethane-based composites with single and dual fillers—carbon and ZnO—prepared under identical conditions to evaluate their combined effect on thermal, dielectric, and surface properties. Unlike previous studies that focused on individual filler performance, this research provides a systematic analysis to determine the most effective composition for coating applications.

## 2. Experimental Methods

### 2.1. Materials

The polyurethane used in this research is a commercially available pure material obtained from an online marketplace without a specific trademark or manufacturer label. Its formulation includes diisocyanate (MDI), MDI-based polyisocyanate, 4,4'-diphenylmethane, aluminum, aromatic solvent blend, and isobutyl acetate. Figure 1 describes groups of the urethane.

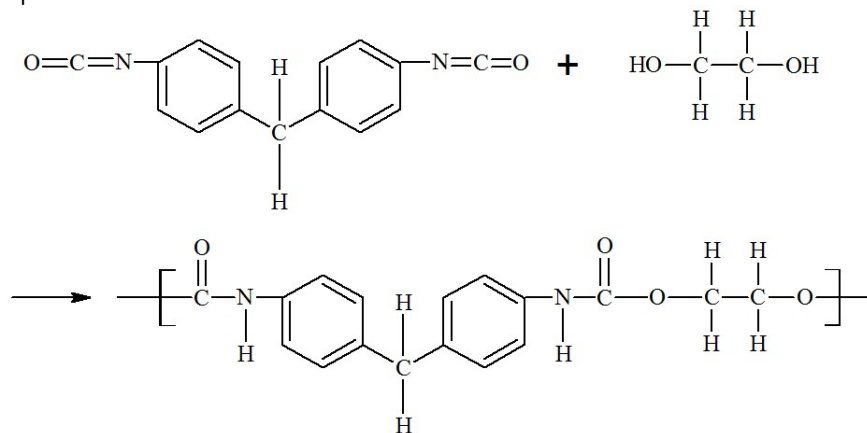


**Figure 1.** Groups of the urethane [9]

Similarly, the nano zinc oxide was synthesized in-house using pure zinc acetate dihydrate ( $Zn(CH_3COO)_2 \cdot 2H_2O$ ) as the precursor through the sol-gel method. The zinc acetate was dissolved in ethanol, stirred at 80 °C for 2 hours to form a gel, then dried at 150 °C for 1 hour, and ground into nanoparticles with an average size of 5 nm. The carbon used was pure graphite powder (30 mesh, ~595 μm), also purchased from the open market without brand identification.

### 2.2. Preparation of Polyurethane Film Composite

#### 2.2.1 Polyurethane/carbon/zinc oxide

The composites were prepared using polyurethane (PU) as the base matrix, mixed separately with carbon, ZnO, and a combination of both fillers. Three types of composites were fabricated: (1) polyurethane/carbon (PC) with 5 wt.% carbon, (2) polyurethane/ZnO (PZnO) with 5 wt.% ZnO, and (3) polyurethane/carbon/ZnO (PCZnO) with a combined filler content of 5 wt.% (carbon and ZnO). The composite composition can be seen in Table 1.

**Table 1.** Composition of sample

Composite sample	No of sample	Filler Composition [wt.%]		Area (mm <sup>2</sup> )	Thickness (mm)
		Micro carbon	ZnO		
PU	1	-	-	415.6	0.35
PC	2	5	-	415.6	0.35
PZnO	3	-	5	415.6	0.35
PCZnO	4	5	5	415.6	0.35

### 2.2.2 Sample Stirring Process

To manufacture the composites, the required amount of filler was weighed according to the designated weight ratio and added gradually into the liquid polyurethane. The mixture was stirred for 120 minutes using a magnetic stirrer (Cimet SP131635, Barnstead Thermolyne, USA) at 500 rpm to achieve uniform dispersion of the fillers within the matrix. Following the mixing process, the composite slurry was applied onto a flat aluminum substrate using the high-volume low pressure (HVLP) spray-coating technique at a pressure of 15 psi. This method was selected to allow uniform deposition of the composite without the use of a vacuum chamber. The coated films were then left to dry under ambient room temperature for 24 hours to complete the curing process and form solid composite layers suitable for characterization [9].

## 2.3. Sequence of Works and Characterization

### 2.3.1 Sequence of Works

The sequence of works is described as Figure 2.

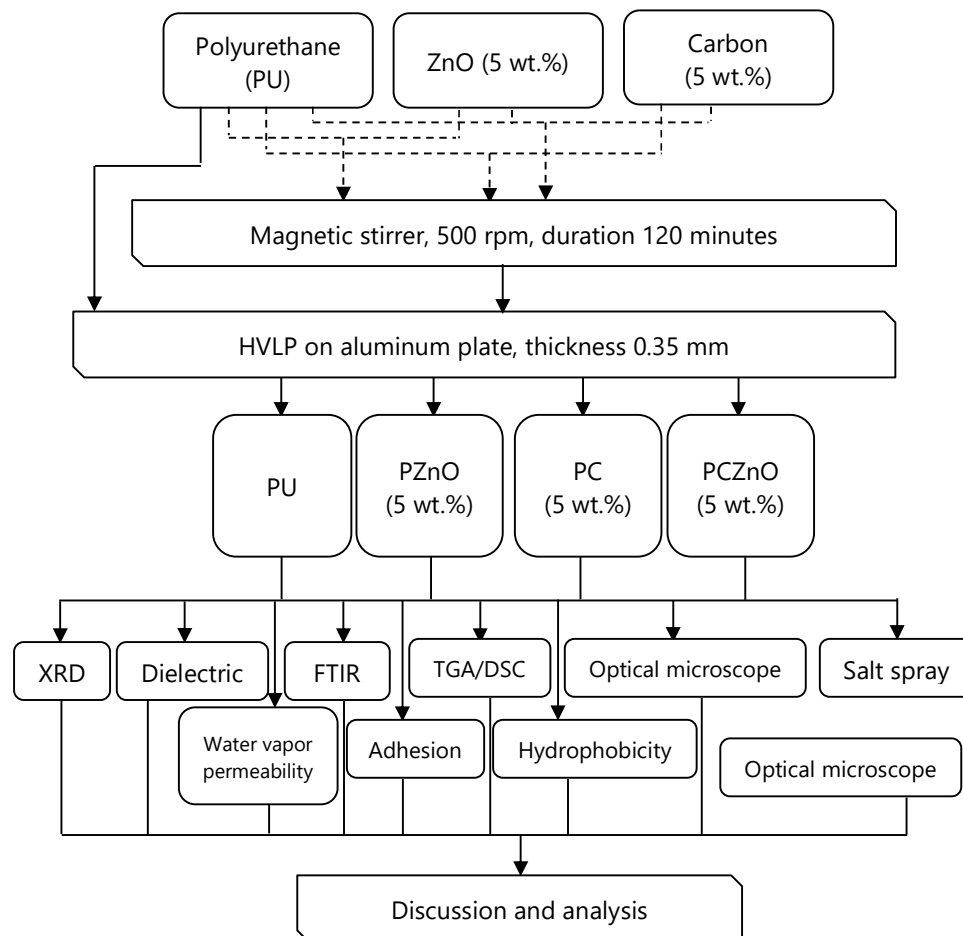


**Figure 2.** Sequence of works

### 2.3.2 Characterization

To identify minerals and phases from the sample X-ray diffraction (XRD), test was carried out. XRD testing uses PANalytical Materials Research Diffractometer (Malvern Panalytical Ltd., UK). The sample size used is 2 × 2 cm which is then exposed at angles 5 - 90°.

Organic substance was identified using the Fourier transform infrared spectroscopy (FTIR) analytical method. In essence, FTIR measures how much of the wavelengths of infrared radiation are absorbed by the item under test. The spectrum two FTIR spectrometer L160000A (Perkin Elmer Inc., USA) was the FTIR apparatus utilized. 2 × 2 cm is the sample size utilized.

Obtaining dielectric properties is done using the capacitance value method. This method is basically through a parallel connection of capacitor mechanism [10]. The sample is placed between 2 aluminum plates and clamped using a clam clip and connected to integrated circuit and to the oscilloscope. Frequency settings are made from 50 kHz to 1 - MHz. Resistance of 11 kΩ is installed as protection. By dividing the permittivity value ( $\epsilon$ ) and by the starting permittivity value in vacuum ( $\epsilon_0$ ), one can determine the dielectric constant ( $\epsilon'$ ).

$$\epsilon' = \frac{\epsilon}{\epsilon_0} \quad (1)$$

The permittivity value is determined by computing capacitance, area, and sample thickness using the fundamental principle since the test results indicate a capacitance value.

$$C = \epsilon \frac{A}{d} \quad (2)$$

where C is capacitance (F),  $\epsilon$  is the permittivity of the material (F/m),  $\epsilon_0$  is the initial permittivity in vacuum ( $8.85 \times 10^{-12} \text{ C}^2/\text{Nm}^2$ ), A is the area of the sample area ( $\text{mm}^2$ ), and d is sample thickness (mm)

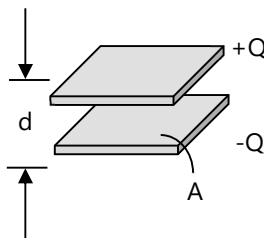


**Figure 3.** Parallel capacitor principle for dielectric test

Thermogravimetry analysis (TGA) and differential scanning analysis are used to determine the mass loss information of the sample during the heating phase. To observe a decomposition process, oxidation, dehydration, or crystallization, the sample's mass loss data is required. TGA and differential scanning calorimetry (DSC) tests are conducted using a 6000 Simultaneous Thermal Analyzer (STA) (Perkin-Elmer Inc., USA) with a test temperature range of 5 to 950 °C.

ASTM B117 [11] standards used to carry out a salt spray test in order to determine the sample's corrosion resistance. A 2 × 2 cm sample was created, and during the 72-hour test, it was sprayed with a 0.5M NaCl solution every three hours. To perform optical microscopy tests, Zeiss Axio Lab. A1 (Carl Zeiss Co., Germany) was utilized. Sample dimensions are 2 × 2 cm, and the image was magnified 100 ×.

Canon 1000D EOS Camer is used to observe the contact angle between liquid and solid surface. The magnitude of the contact angle is compared to the criteria in Figure 4.

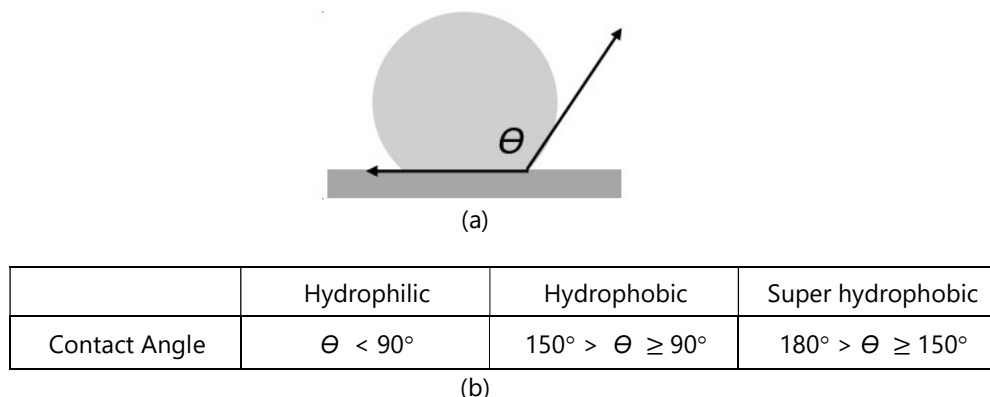


**Figure 4.** (a) Contact angle (b) hydrophobicity criteria

### 3. Results and Discussion

#### 3.1. XRD analysis

The XRD analysis is used to identify compositions and phases of composite, therefore four samples for XRD tests were chosen such as PC, PZnO, PCZnO, and PU. The PU is a control parameter.

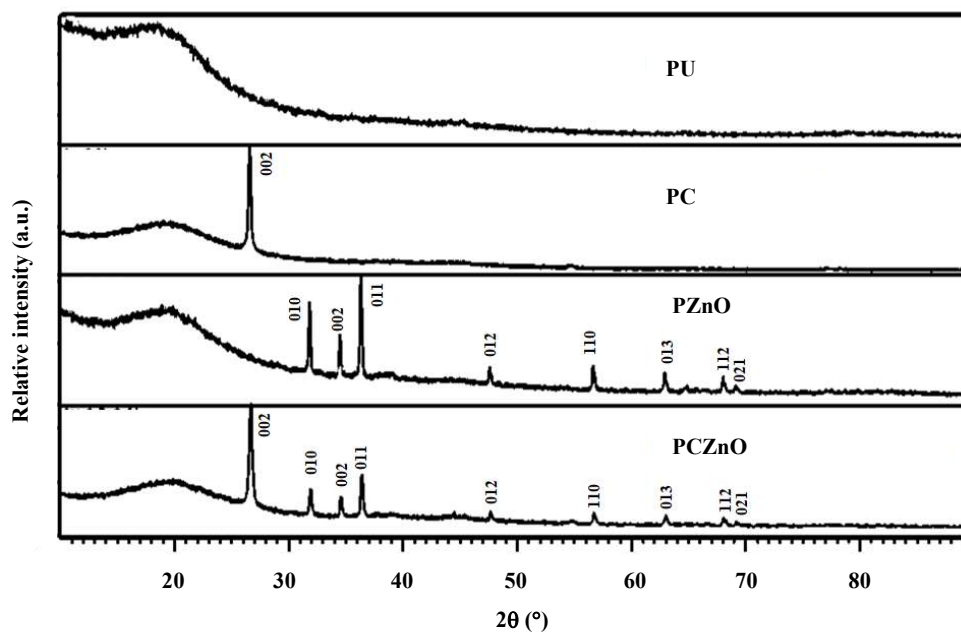


**Figure 5.** Result of XRD for polyurethane/Carbon/ZnO

Figure 5 shows that polyurethane phase forms are in the range of 10 - 25° and the result of the graph is a typical form of XRD graph on polymer material. PC has 1 phase peaks identified on the graph, namely 002 with angular positions of 27°. PZnO composite has a total of 8 peaks are 010, 002, 011, 012, 110, 013, 112, and 021 with positions of 32, 34, 36, 48, 57, 63, 68, and 69° respectively. While the PCZnO composite has a total of 9 phase peaks identified on the graph which are the combined results of the graphite and ZnO phases. The hkl index and angular position shown in the PCZnO graph are the same as those shown in the PC and PZnO charts.

The XRD results confirm the successful incorporation of carbon and ZnO into the polyurethane matrix, as evidenced by the distinct diffraction peaks associated with each filler. The increase in the number of phase peaks

in the PCZnO composite indicates the presence of both filler phases without significant interference. This observation agrees with previous studies [8], which reported that ZnO and carbon fillers tend to retain their crystalline structure when embedded in polymer matrices. The well-defined peaks suggest good compatibility between the fillers and polyurethane, which can contribute to enhanced thermal and mechanical properties.

### 3.2. Thermogravimetry (TGA) analysis

The application of Thermogravimetry analysis test is to get information about mass loss from the test sample when loaded with heat in a certain period, so that the decomposition process of the sample can also be seen. Figure 5 is the TGA curve of the composite sample tested.

There are two stages to the sample's decomposition process when heated: the first stage affects the urethane chain's hard segment (isocyanate), and the second stage starts to alter or break the bond of a polyurethane soft segment (polyol) chain made up of the bonds -CH and -OH. The first stage decomposition for PC composites occurs at around temperatures 302 - 405°C and the second stage, the values of was 585 and 800°C, respectively. For PZnO composites for the first stage 332 - 420°C and for second stage decomposition values of samples around 600°C. The PCZnO composites have almost the same values as the first stage around 338 - 442°C. In the second stage, it showed great results indicated by very stable condition when the heating temperature arrived at a maximum temperature of 800°C. This is consistent with the research carried out previously that the addition of ZnO has a positive effect for thermal decomposition in soft segments [8].

Figure 6 shows the TGA curve of several composites have the best thermal decomposition of various samples. Composite carbon/polyurethane with a carbon content shows the best decomposition from other composite samples.

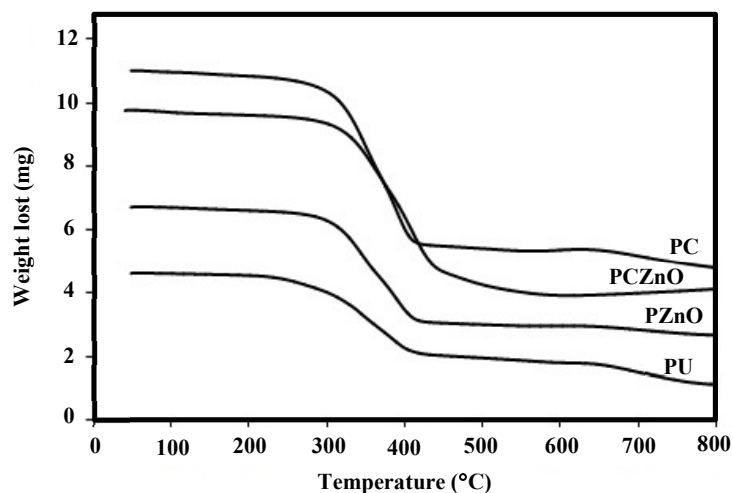


**Figure 6.** TGA curve of PC, PZnO, and PCZnO composite

These findings are in line with previous studies [8] that reported enhanced thermal stability in polyurethane composites with ZnO fillers is due to their ability to improve heat resistance by restricting polymer chain mobility. The observed higher decomposition temperatures in PCZnO composites confirm the synergistic role of both fillers in enhancing thermal degradation resistance.

### 3.3. Differential Scanning Calorimetry (DSC)

Tests related to the stability of the material to temperature are carried out through DSC by looking at the pattern of heat flow in the temperature function. Besides testing the decomposition and stability of the material against temperature changes, it is also necessary to know what bonding groups will decompose first or not decompose at all. The chain's crosslinking will have an impact on the temperature response. Thermal transitions

occur at high temperatures because crosslinking reduces chain flexibility and prevents polymer chains from moving, causing a shift in the melting and crystallization temperatures [12], [9].

Figure 7 shows DSC curve of composites. PC sample shows sudden decrease in heat flow around 300°C but steady. PU and PZnO composite show sudden decrease in heat flow around 800°C. The PCZnO composite shows a better thermal stability than others.

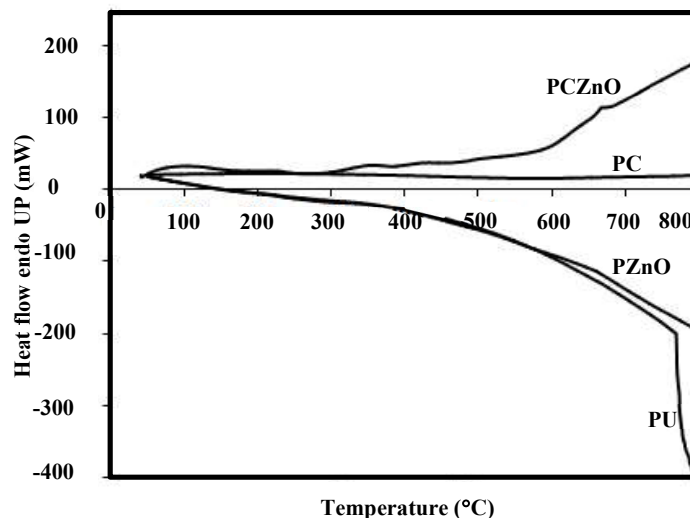


**Figure 7.** DSC curve of composites

The shift in heat flow patterns, especially in PCZnO, suggests enhanced crosslinking density and reduced chain flexibility, consistent with findings by Sattar et al. [12]. This supports the conclusion that the addition of dual fillers modifies the thermal transition behavior and stabilizes the composite structure at elevated temperatures.

### 3.4. Fourier Transform Infrared (FTIR) Analysis

FTIR analysis was applied to identify functional group of composites. Figure 8 shows FTIR spectrum of sample. In the spectrometer all types of composites frequency —OH and —NH occur around the peak 3200 - 3300  $\text{cm}^{-1}$ . The frequency of C—H is around the wave number 3000  $\text{cm}^{-1}$ . Double bonds such as frequencies C=O, C=C, and C=N at peak 1500 - 1400  $\text{cm}^{-1}$ . For vibrations from C—O—C bonds as a characteristic of urethane chains, there are frequencies of around 1000-1100  $\text{cm}^{-1}$  and for vibrations of aromatic chains C=C—C and C—H each at 1597  $\text{cm}^{-1}$  and 1200  $\text{cm}^{-1}$  [12]. There is a relationship between transmittance and wave number; for wave numbers between 500 and 4000  $\text{cm}^{-1}$ , pure polyurethane has the best transmittance. The N-H and O-H links in Figure 8 are located between 3200 and 3400  $\text{cm}^{-1}$  and 1600 and 1700  $\text{cm}^{-1}$ , respectively, which shows a hydrogen bond. Figure 8 shows the N-H region of the urethane chain in the PC at additional peaks that show the presence of carbon bonds. The PZnO composite's FTIR spectrometer is shown in Figure 7. The research indicates that N-H and C=O bonds on wave numbers 3521  $\text{cm}^{-1}$  and 1592  $\text{cm}^{-1}$  have the greatest influence on ZnO fill material [13]. Figure 8 represent of FTIR curve from several composites which have the best stronger bond of several types of composites. Composite PZnO is the strongest.

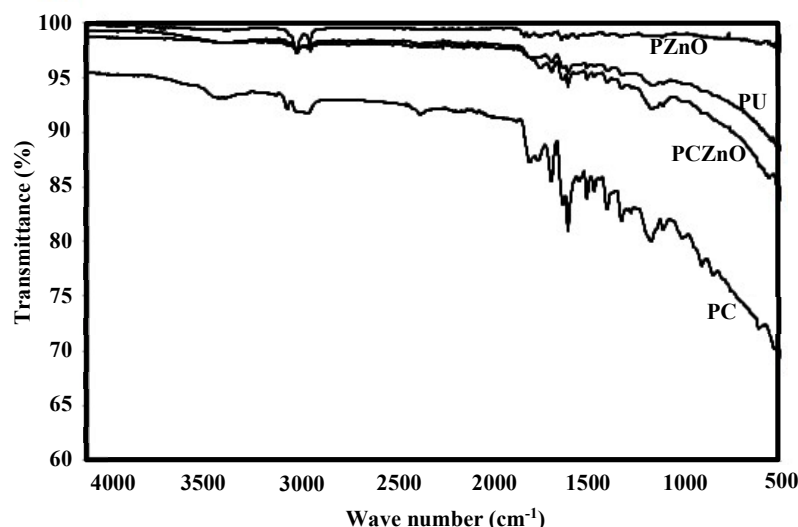


**Figure 8.** FTIR curve of composites

The identification of characteristic peaks and stronger bond intensities in the composites aligns with previous observations [13], where ZnO improved hydrogen bonding and interaction with polymer chains. The spectrum differences between PC and PZnO further support that the fillers contribute differently to the molecular structure of polyurethane.

### 3.5. Corrosion Resistance analysis

In many sectors, long-lasting corrosion protection is vital. Particularly, steel constructions—such as sheet pile walls, breakwater structures, water gates, dams, and barrages—are subjected to water consistently. High-quality raw-material-based elastic polyurethane coating is required. Salt spray was used on PU with varying carbon concentrations. Before and after the salt spray test to determine the sample’s corrosion resistance characteristics, the surface morphology is displayed in the accompanying figure.

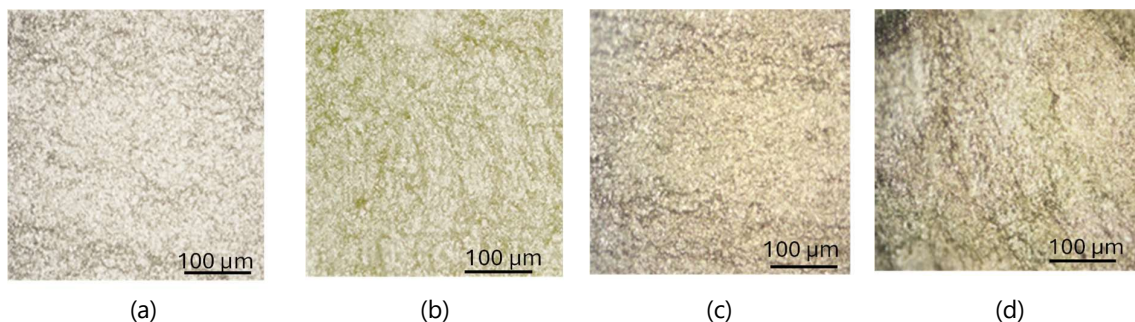


**Figure 9.** Surface morphology of composites before corrosion (a) PU 100x, (b) PC 100x, (c) PZnO 100x, and (d) PCZnO 100x

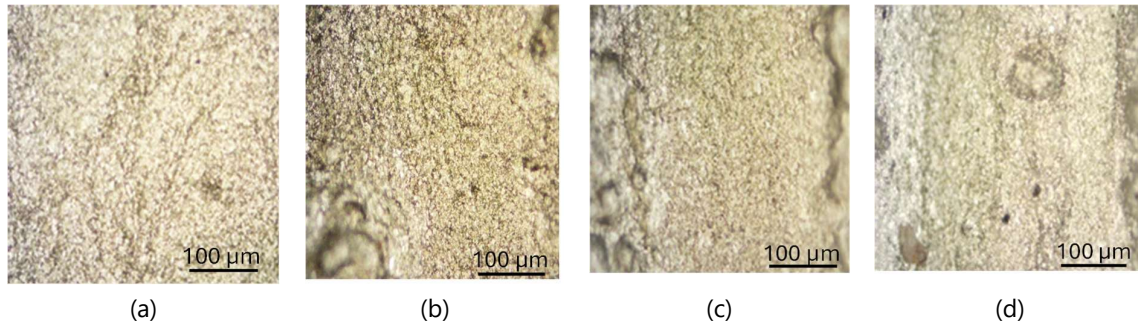


**Figure 10.** Surface morphology of composites after corrosion (a) PU 100×, (b) PC 100×, (c) PZnO 100×, and (d) PCZnO 100×

Figures 9 and 10 show the results of corrosion tests observed using an Optical Microscope (OM). From visual data, the surface morphology of the composite layer occurs a lot of deposits, especially for PZnO and PCZnO composites. PU showed good results. These deposits occur due to agglomeration on the surface of the layer. Another observation is that there are also many porous or holes in each composite. This is a response to corrosion that attacks the surface of the layer through oxidation reactions [14].

The results are consistent with corrosion studies on nanocomposite coatings, where ZnO nanoparticles did not only provide partial barrier properties but also introduced agglomeration that increased localized corrosion [15]. The difference in deposit and pore formation compared to pure PU supports this interpretation and highlights the trade-off between filler dispersion and corrosion behavior.

### 3.6. Dielectric Analysis

Barrier analysis method is carried out to conduct a dielectric properties test. A Specimen as an electrochemical cell content putted like sandwich as layered between two aluminum plate [16]. The data obtained is in the form of dielectric constant values to identify the dielectric properties of the samples composite. The value of this dielectric constant is obtained from the results of the conductive network in the test specimen material and the capacitor effect between plat which filled by composite [15]. Figure 11 below shows the graph of the relationship of AC frequency with the dielectric constant value tested at room temperature. The overall analysis of the carbon filing results will influence the best permittivity as show Figure 11. PCZnO composite is not mentioned in Figure 11 due to lack of data result.

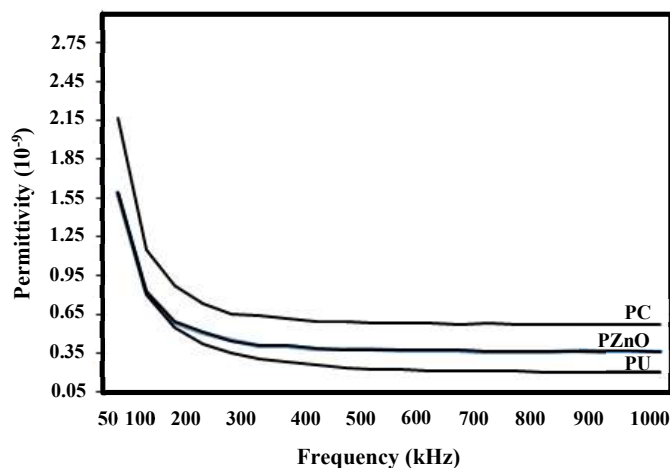


**Figure 11.** The best permittivity of composites

The increase in dielectric constant for carbon-filled samples agrees with prior work [15], which attributed such enhancements to conductive network formation and interfacial polarization within the matrix. The absence of PCZnO data limits direct comparison, but the trend confirms carbon's dominant influence on dielectric performance.

### 3.7. Hydrophobicity Analysis

Observations on all samples related to the nature of hydrophobicity showed that all samples have hydrophobic properties (see Figures 12,13,14, and 15). Observation of the contact angle for polyurethane formed angle 44,52,53, and 45°. Meanwhile, the contact angle between liquid and solid surface for polyurethane carbon is 50, 57, 63, and 58°.



Figure 12. Contact angle of PU samples

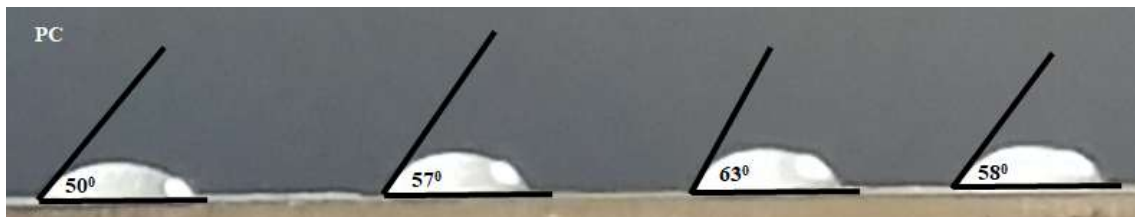


Figure 13. Contact angle of PC samples



Figure 14. Contact angle of PZnO samples



Figure 15. Contact angle of PCZnO samples

**Table 2.** Contact angle observation result of composite

No.	Film composite	Contact angle (°)				Average (°)
		Sample 1	Sample 2	Sample 3	Sample 4	
1	PU	44	52	53	45	48.5
2	PC	50	57	63	58	57.00
3	PZnO	47	48	48	47	47.67
4	PCZnO	38	38	38	36	37.50

Table 2 shows composites containing ZnO decrease the contact angle, otherwise composite filled by carbon increases contact angle. The results agree with prior literature [13] that reported increased hydrophobicity with carbon additives is due to surface roughness and nonpolar interactions. In contrast, the lower contact angles in ZnO-containing composites may result from increased surface polarity and potential filler agglomeration.

### 3.8. Adhesion Analysis

ASTM D3399 was applied to conduct adhesion tests. A comparison is made between the test result and the standard classification.

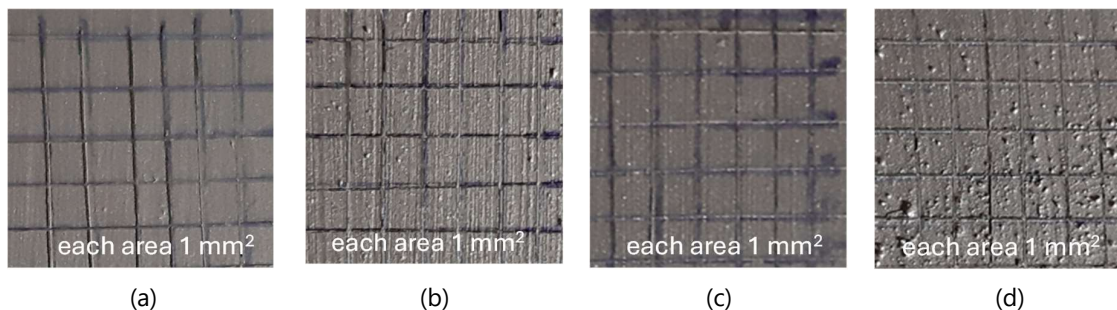


**Figure 16.** Surface of composite after adhesion test (a) PU, (b) PC, (c) PZnO, and (d) PCZnO

Figure 16 shows that all result adhesion test included to 5B classification. It means that result of the adhesion test is excellent with the ASTM D3359 standard. The outstanding adhesion (5B rating) across all composites aligns with previous research [9], which demonstrated that polyurethane maintains strong interfacial bonding with metallic substrates regardless of filler type. It is likely due to its flexible chain structure and good substrate compatibility.

### 3.9. Water Vapor Permeability

It is anticipated that the outcomes of the water vapor permeability test will give a summary of the composite materials with the highest water vapor permeability among the evaluated samples. Figure 17 shows the weight of water vapor absorbed by silica gel as a metric of the composite's water vapor permeability.

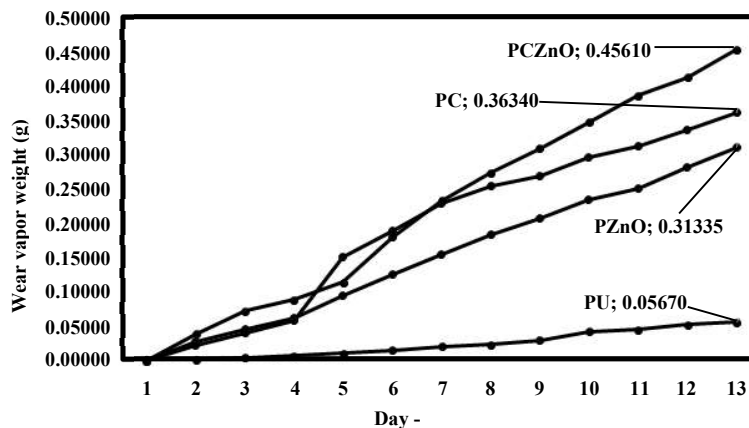


**Figure 17.** Surface of composite after adhesion test

It is seen that the addition of carbon concentration to polyurethane increases the absorption of moisture from composite. This confirms the results of the salt spray test that increasing the carbon content in polyurethane further increases corrosion. Figure 18 describes that the addition of carbon, ZnO and carbon/ZnO in polyurethane matrix are increasing water vapor absorption. It is assumed that the increasing of water vapor permeability is due to agglomeration.

These results corroborate previous findings [6] that increased filler loading, particularly with carbon, can enhance moisture uptake due to micro-void formation and agglomeration. The increased permeability in ZnO and PCZnO composites may also indicate suboptimal dispersion, as suggested in other nanocomposite studies [8].

### 3.10. Result of Characterization in Term of Composite as a Coating Material Purposes

Based on the results of the characterization was carried out, scores were then made to obtain the best material as a coating material. Score 0 it is mean poor, 1 for fair, 2 for good and 3 for very good.

**Table 3.** Scoring table

Characterization	Composites			
	PU	PC	PZnO	PCZnO
TGA	0	3	1	2
DSC	0	2	1	3
FTIR	2	0	3	1
Salt spray	3	1	0	2
Hydrophobicity	2	3	1	0
Adhesion	3	3	3	3
Water vapour permeability	3	1	2	2
Dielectric	0	3	2	2
Total score	13	16	13	13

Scoring in Table 3 shows that PC is the best composite to use as a coating material purposes. The scoring results are consistent with the individual test findings and support conclusions from similar works [7], where carbon-enhanced composites performed better overall in thermal and electrical domains. The performance trade-offs observed for PCZnO suggest that dual-filler systems require optimized ratios and improved dispersion techniques to outperform single-filler composites.

#### 4. Conclusion

This study has successfully characterized polyurethane composites filled with carbon, zinc oxide, and their combination to assess their potential as coating materials. The PC composite demonstrated the highest thermal stability with decomposition stages occurring at 302–405°C and 585–800°C, respectively. FTIR analysis confirmed the presence of functional groups such as N–H and C=O, while DSC results indicated better thermal resistance in PCZnO composites. The dielectric constant of the carbon-filled composite reached a maximum of 8.1 at 100kHz, showing strong insulation properties. In corrosion testing, PZnO and PCZnO samples exhibited increased surface deposits and porosity, suggesting higher susceptibility to salt spray exposure. Contact angle measurements confirmed hydrophobicity in all samples, with the PC composite achieving the highest angle of 63°, indicating superior water repellency. Furthermore, all samples achieved a 5B classification in adhesion testing based on ASTM D3359 standards, and water vapor permeability increased by approximately 15% with carbon addition. Overall, the polyurethane/carbon composite was quantitatively identified as the best candidate for coating applications based on its superior performance across thermal, dielectric, and surface property parameters.

#### 5. Acknowledgments

The author acknowledges with gratitude the financial support from the Ministry of Research, Technology and Higher Education of Indonesia (RISTEK-DIKTI), under grant Hibah Penelitian Doktor.

#### 6. References

- [1] S. Y. Moon, J. K. Kim, C. Nah, and Y. S. Lee, "Polyurethane/montmorillonite nanocomposites prepared from crystalline polyols, using 1,4-butanediol and organoclay hybrid as chain extenders," *Eur Polym J*, vol. 40, no. 8, pp. 1615–1621, 2004, doi: 10.1016/j.eurpolymj.2004.04.018.
- [2] A. Sorrentino, G. Gorrasi, M. Tortora and V. Vittoria, "Barrier properties of polymer/clay nanocomposites," in *Polymer Nanocomposites*, Woodhead Publishing, pp. 273–296, 2006.
- [3] A. K. Barick and D. K. Tripathy, "Thermal and dynamic mechanical characterization of thermoplastic polyurethane/organoclay nanocomposites prepared by melt compounding," *Materials Science and Engineering A*, vol. 527, no. 3, pp. 812–823, 2010, doi: 10.1016/j.msea.2009.10.063.
- [4] D. Sarkar and S. T. Lopina, "Oxidative and enzymatic degradations of L-tyrosine based polyurethanes," *Polym Degrad Stab*, vol. 92, no. 11, pp. 1994–2004, 2007, doi: 10.1016/j.polymdegradstab.2007.08.003.
- [5] V. Melnig, M. O. Apostu, V. Tura, and C. Ciobanu, "Optimization of polyurethane membranes: Morphology and structure studies," *J Memb Sci*, vol. 267, no. 1–2, pp. 58–67, 2005, doi: 10.1016/j.memsci.2005.04.054.
- [6] E. Ciecierska *et al.*, "Flammability, mechanical properties and structure of rigid polyurethane foams with different types of carbon reinforcing materials," *Compos Struct*, vol. 140, pp. 67–76, 2016, doi: 10.1016/j.compstruct.2015.12.022.
- [7] P. S. Goh, A. F. Ismail, and B. C. Ng, "Directional alignment of carbon nanotubes in polymer matrices: Contemporary approaches and future advances," *Compos Part A Appl Sci Manuf*, vol. 56, pp. 103–126, 2014, doi: 10.1016/j.compositesa.2013.10.001.
- [8] J. Pavličević *et al.*, "The influence of ZnO nanoparticles on thermal and mechanical behavior of polycarbonate-based polyurethane composites," *Compos B Eng*, vol. 60, pp. 673–679, 2014, doi: 10.1016/j.compositesb.2014.01.016.
- [9] O. Kurniawan and B. Soegijono, "Preparation and characterization of polyurethane/carbon/organoclay composite for coating of aluminum conductor overhead lines," vol. 18, pp. 62–69, 2020, doi: 10.1380/ejsnt.2020.62.
- [10] I. Piekarz, J. Sorocki, and M. Bozzi, "Test tube dedicated microwave liquid dielectric sensor for non-contact properties change monitoring and material characterization with tube exchange capability," *Measurement (Lond)*, vol. 198, 2022, doi: 10.1016/j.measurement.2022.111397.

- 
- [11] Anon, "Standard method of salt spray (fog) testing," *ASTM Special Technical Publication*, pp. 496–504, 1985.
- [12] R. Sattar, A. Kausar, and M. Siddiq, "Thermal, mechanical and electrical studies of novel shape memory polyurethane/polyaniline blends," *Chin J Polym Sci*, vol. 33, pp. 1313–1324, 2015, doi: 10.1007/s10118-015-1680-5.
- [13] A. Z. Okkema, D. J. Fabrizio, T. G. Grasel, S. L. Cooper, and R. J. Zdrahala, "Bulk, surface and blood-contacting properties of polyether polyurethanes modified with polydimethylsiloxane macroglycols," *Biomaterials*, vol. 10, no. 1, pp. 23–32, 1989, doi: 10.1016/0142-9612(89)90005-7.
- [14] E. M. Richter, G. Possart, P. Steinmann, S. Pfaller, and M. Ries, "Revealing the percolation–agglomeration transition in polymer nanocomposites via MD-informed continuum RVEs with elastoplastic interphases," *Compos B Eng*, vol. 281, p. 111477, 2024, doi: 10.1016/j.compositesb.2024.111477.
- [15] H. Sun *et al.*, "Interfacial polarization and dielectric properties of aligned carbon nanotubes/polymer composites: the role of molecular polarity," *Compos Sci Technol*, vol. 154, pp. 145–153, 2018, doi: 10.1016/j.compscitech.2017.11.008.
- [16] T. C. Wen, S. L. Hung, and M. Digar, "Effect of polypyrrole on the morphology and ionic conductivity of TPU electrolyte containing LiClO<sub>4</sub>," *Synth Met*, vol. 118, no. 1–3, pp. 11–18, 2001, doi: 10.1016/S0379-6779(00)00272-1.